

Emission control by binary energy transfer processes on oligouridine

Shuji Ikeda,^a Takeshi Kubota,^a Dan Ohtan Wang,^{a,b} Hiroyuki Yanagisawa,^a Mizue Yuki^a and Akimitsu Okamoto^{*a,c}

Received 1st June 2011, Accepted 27th June 2011

DOI: 10.1039/c1ob05869j

Fluorescent oligonucleotides have been designed on which two different energy transfer processes were mounted together: excitonic interaction and FRET. The fluorescence emission of the oligonucleotides was controlled well by the two different energy transfer processes, in response to their hybridization to the complementary RNA both *in vitro* and in cells.

Introduction

Energy transfer phenomena continue to fascinate many chemists, biologists, and physicists, and the literature contains numerous experiments designed to demonstrate and apply energy transfer to each research field.¹ Such energy transfer processes provide us with significant information about the distance, orientation, and interaction between two dyes, based on the intensities and wavelength shifts of the absorption and emission, which can be classified into several types depending on the coupling strength between the dyes. One of the most familiar energy transfer processes is Förster resonance energy transfer (FRET). FRET is a vibrational–relaxation resonance transfer between the excited states of two dyes, in which the excitation is transferred from a donor to an acceptor without the emission of a photon, with inverse sixth-power dependence on the distance between the fluorescent dyes.^{1,2} FRET is now an important technique for investigating a variety of biological phenomena that produce changes in molecular proximity. Another energy transfer process, the exciton model, is defined as the resonance interaction between the excited states of loosely bound dye aggregates.^{1,3} Recently, the interdy excitonic interaction has been applied to the detection of nucleic acids.⁴ The excitonic interaction is characterized by large differences between the absorption spectrum of the dye aggregate and those of its components, and shows a high resonance transfer rate, dependent on the inverse cube of the distance between the fluorescent dyes. To the best of our knowledge, these energy transfers have not yet been used together for the analysis of interactive biomolecules. However, the combination of such energy transfer processes should provide us with more information on molecular structures and interactions than single energy transfer processes do.

In this paper, two such energy transfer processes were mounted on one oligonucleotide, which provided us with valuable information about its hybridization with RNA. The use of the oligonucleotide as a hybridization-sensitive fluorescent probe to image the intracellular poly(A)⁺ RNA effectively provided much information on the distribution of the fluorescence-labeled probe and the localization of poly(A)⁺ RNA in a living cell.

Results and discussion

Design and synthesis

We synthesized fluorescent nucleic acids so that their emission could be controlled by excitonic interaction and FRET (Fig. 1). A doubly fluorescent-dye-labeled nucleotide, D₅₁₄, that generates an exciton interaction was incorporated into an oligonucleotide. The synthetic oligonucleotide, called an exciton-controlled hybridization-sensitive fluorescent oligonucleotide (ECHO) probe, emits fluorescence only when it hybridizes with the complementary nucleic acid.^{4a,b} The ECHO probes used in this study were equipped with a 2'-*O*-methyl ribonucleotide (except D₅₁₄), which forms a thermostable hybrid with the complementary RNA and has nuclease resistance.⁵ Moreover, an intramolecular FRET donor/acceptor pair was designed by the attachment of a 'stationary' fluorescent dye, Cy5, to the end of the ECHO probes: 5'-Cy5-s-s-U_nD₅₁₄U₆-3', where 's' is a hexaethylene glycol linker and *n* is 2, 5, 10, or 15 (Table 1). The sequence used for the probe was oligo(2'-*O*-methyluridine), which can be used to label poly(A) sequences such as mRNA poly(A) tail.^{4c} The distance between the ECHO nucleotide and the stationary fluorescent dye was controlled by the number of 2'-*O*-methyluridines inserted between the dyes.

Photophysics *in vitro*

The absorption band of Cy5 on the probe end was observed at the original absorption wavelength, 645 nm (Fig. 2a). In contrast, the absorption band of D₅₁₄, a nucleotide labeled with two thiazole orange dyes, showed the photophysical behavior characteristic of

^aAdvanced Science Institute, RIKEN, Wako, Saitama, 351-0198, Japan. E-mail: aki-okamoto@riken.jp; Fax: +81 48 467 9205; Tel: +81 48 467 9238

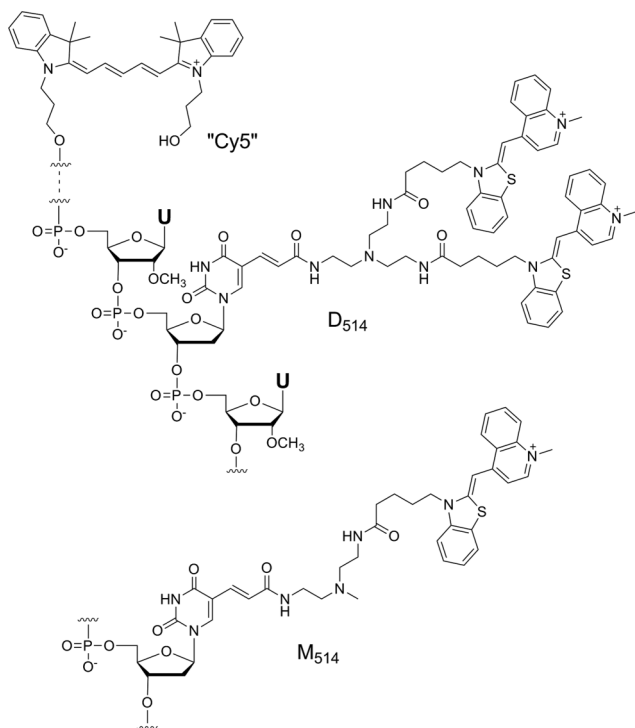
^bInstitute for Integrated Cell-Material Sciences (iCeMS), Kyoto University, Yoshida Ushinomiya-cho, Sakyo-ku, Kyoto, 606-8501, Japan

^cPRESTO, Japan Science and Technology Agency, 4-1-8 Honcho, Kawaguchi, Saitama, 332-0012, Japan

Table 1 Mass and photophysical data of the probes

D ₅₁₄ /Cy5 probes ^a	MALDI-TOF Mass ^b	Calcd	Found	T _m (°C)	ε ₄₇₆ (dm ³ mol ⁻¹ cm ⁻¹)	ε ₅₀₇ (dm ³ mol ⁻¹ cm ⁻¹)	ε ₆₄₅ (dm ³ mol ⁻¹ cm ⁻¹)	I ₅₄₄ ^c	I ₆₆₃ ^c	E ^d
Cy5-s-s-U ₁₅ D ₅₁₄ U ₆	[M - 2H] ⁺	9117.8	9118.5	59	69 000	42 000	150 000	0.25	9.8	—
					43 000	76 000	170 000	19	15	0.66
Cy5-s-s-U ₁₀ D ₅₁₄ U ₆	[M - 2H] ⁺	7516.7	7516.6	52	89 000	58 000	180 000	0.11	16	—
					51 000	92 000	190 000	7.5	25	0.87
Cy5-s-s-U ₅ D ₅₁₄ U ₆	[M - 2H] ⁺	5915.8	5916.0	40	86 000	47 000	170 000	0.031	19	—
					51 000	88 000	200 000	5.1	28	0.91
Cy5-s-s-U ₂ D ₅₁₄ U ₆	[M - 2H] ⁺	4955.2	4956.2	34	81 000	47 000	110 000	0.051	16	—
					52 000	73 000	110 000	1.7	21	0.97
Cy5-s-s-U ₂₂	M ⁺	8204.6	8203.7	54	—	—	220 000	—	0.37	—
					—	—	220 000	—	0.36	—
U ₁₅ D ₅₁₄ U ₆	[M - H] ⁺	7896.6	7896.9	58	83 000	58 000	—	0.47	—	—
					50 000	93 000	—	56	—	0
Cy5-s-s-U ₁₅ M ₅₁₄ U ₆	[M - H] ⁺	8716.2	8716.4	59	12 000	26 000	150 000	0.008	2.9	—
					14 000	33 000	160 000	5.8	6.4	0.69
U ₁₅ M ₅₁₄ U ₆	M ⁺	7495.0	7494.7	60	8800	21 000	—	0.42	—	—
					8500	25 000	—	19	—	0

^a "U" and "s" in probe sequences denote a 2'-O-methyluridine and a hexaethylene glycol linker, respectively. ^b MALDI-TOF mass spectroscopic data. Here, the molecular weight of the counter anions of dyes is not included in the value of M of the molecules including D₅₁₄, M₅₁₄, or Cy5. ^c Excitation wavelength was 488 nm. ^d FRET efficiency. The fluorescence intensities of U₁₅D₅₁₄U₆ and U₁₅M₅₁₄U₆ were used for the standard fluorescence intensities of the FRET donor (I_D) of D₅₁₄/Cy5 and M₅₁₄/Cy5 systems, respectively. ^e ss, unhybridized (single-stranded); ds, hybridized with poly(A) RNA (double-stranded).

**Fig. 1** Structures of binary energy transfer oligonucleotides.

interdye excitonic interaction.^{3,6} An absorption band at 476 nm appeared more strongly when the probe was in an unhybridized state, whereas an absorption band at 507 nm became predominant when the probe was hybridized with poly(A) RNA. The excitonic interaction between D₅₁₄ thiazole orange dyes causes a splitting of the excited state of dyes into two energy levels, E' (the out-of-phase dipole arrangement) and E'' (the in-phase dipole interaction), and transitions from the ground state to exciton state E' are

forbidden, while transitions from the ground state to exciton state E'' are allowed (Fig. 3).³ Therefore, the absorption wavelength of the unhybridized probe was shorter. On the other hand, after hybridization, the dye interaction is lost by binding of each dye to the duplex structure.⁴ Therefore, the absorption band of D₅₁₄ in the hybrid appeared at the original absorption wavelength of thiazole orange.

The fluorescence emission of the probes was controlled well by the two different energy transfer processes, depending on the hybridization of the probes to the complementary RNA. The D₅₁₄/Cy5 system, Cy5-s-s-U₁₅D₅₁₄U₆, which was hybridized with poly(A) RNA, showed fluorescence emission at the emission wavelength of D₅₁₄ (544 nm), whereas the emission intensity was almost negligible before hybridization (Fig. 2b). The switching of the fluorescence intensity at 544 nm can be accepted as a general feature of the controlled excitonic interaction.^{4,7} In the exciton model, radiative transitions from E' to the ground state are formally forbidden after the rapid internal conversion from E'' to E' (Fig. 3).³ Consequently, the fluorescence emission from the unhybridized probe was strongly suppressed.

Another D₅₁₄/Cy5 system, Cy5-s-s-U₂D₅₁₄U₆, which has fewer uridines between the dyes, showed strong suppression of the emission at 544 nm, even when hybridized with the poly(A) RNA (Fig. 2b). In contrast, the fluorescence intensity at 663 nm with excitation at 488 nm was higher than that of the hybrid between Cy5-s-s-U₁₅D₅₁₄U₆ and the poly(A) RNA, suggesting that the energy transfer from D₅₁₄ to Cy5 in Cy5-s-s-U₂D₅₁₄U₆ occurred more efficiently. The FRET efficiencies of Cy5-s-s-U_nD₅₁₄U₆/poly(A) RNA duplexes were 66%, 87%, 91% and 97% for n = 15, 10, 5 and 2, respectively (Table 1), and the Förster radius (R₀) calculated for them was 5.1 nm. The R₀ of the D₅₁₄/Cy5 system was almost the same as that of the M₅₁₄/Cy5 system (R₀ = 5.2 nm), which was labeled with only one thiazole orange dye (Fig. 1).^{4b,8} This means that each thiazole orange dye of D₅₁₄ in the hybridized

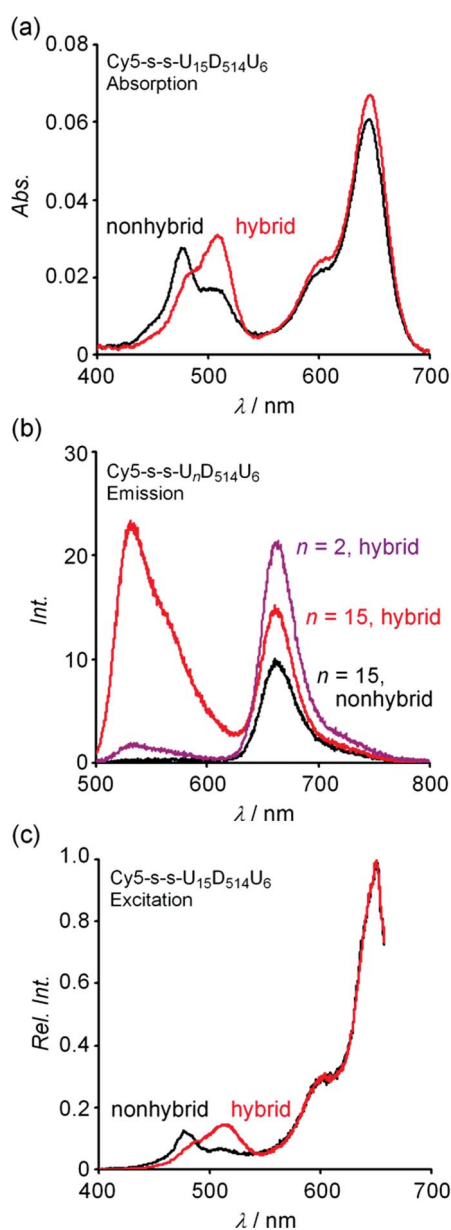


Fig. 2 Photophysics of the binary energy transfer oligonucleotides. (a) Absorption spectra of $\text{Cy5-s-s-U}_{15}\text{D}_{514}\text{U}_6$ before and after hybridization with poly(A) RNA. (s = hexaethylene glycol). (b) Emission spectra of $\text{Cy5-s-s-U}_{15}\text{D}_{514}\text{U}_6$ and $\text{Cy5-s-s-U}_2\text{D}_{514}\text{U}_6$. The excitation wavelength was 488 nm. (c) Excitation spectra of $\text{Cy5-s-s-U}_{15}\text{D}_{514}\text{U}_6$ before and after hybridization with poly(A) RNA. The spectra were collected for emission at 663 nm.

probe independently participates in FRET because the excitonic interaction between the two dyes of D_{514} was disrupted in the hybrids with RNA and the dyes intercalated independently into the duplex structure.

Unhybridized $\text{Cy5-s-s-U}_{15}\text{D}_{514}\text{U}_6$ also showed emission at 663 nm with excitation at 488 nm, although the emission at 544 nm was strongly suppressed by the excitonic interaction between the dyes of D_{514} . The excitation spectra of unhybridized $\text{Cy5-s-s-U}_{15}\text{D}_{514}\text{U}_6$ collected at the Cy5 emission wavelength showed a signal at 476 nm (Fig. 2c), indicating that the FRET process from the split excited state was present in the unhybridized form. The

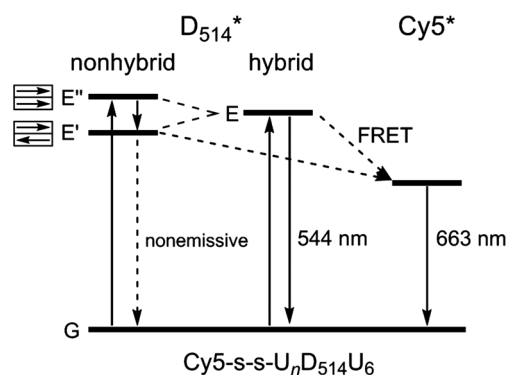


Fig. 3 Schematic representation of the energy levels of the unhybridized and hybridized probes controlled by excitonic interaction and FRET.

split excited state of the dye aggregate makes the dye nonemissive in an exciton model because the transition is forbidden,^{3,4b} whereas it can be the donor for FRET and contribute to the acceptor emission at a longer wavelength (Fig. 3).

Binary photoprocess probes in cells

The double energy transfer system may be applicable to RNA imaging and may provide a way to simplify a lot of complicated information that is generated in the presence of both the fluorescent probe and the target RNA in a cell, including the presence of the target RNA, the probe distribution, and the RNA localization (Fig. 4a). We microinjected a poly(A)⁺ RNA-targeting $\text{D}_{514}/\text{Cy5}$ probe, $\text{Cy5-s-s-U}_2\text{D}_{514}\text{U}_6$, which was shown to have high FRET efficiency in an *in vitro* assay as described above, into the nuclei of two living HeLa cells. The cell nuclei emitted strong

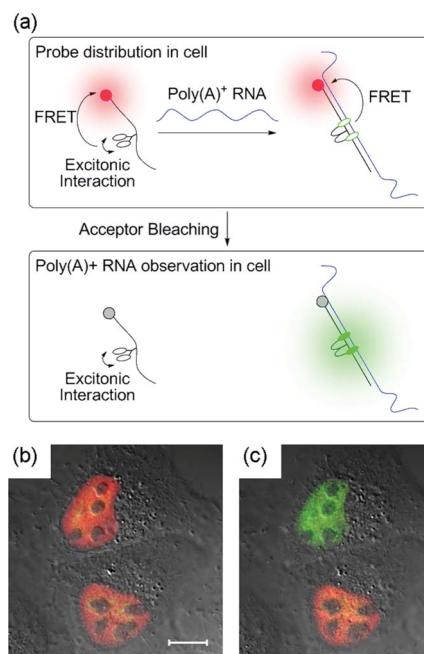


Fig. 4 Acceptor bleaching. (a) Hybridization-dependent binary energy transfer control. (b) An image of $\text{Cy5-s-s-U}_2\text{D}_{514}\text{U}_6$ -injected HeLa cells before bleaching. Bar, 10 μm . Green, fluorescence through a 505–550 nm filter; red, fluorescence through a 625–722 nm filter. (c) An image after only the nucleus of the top cell was scanned repeatedly at 633 nm.

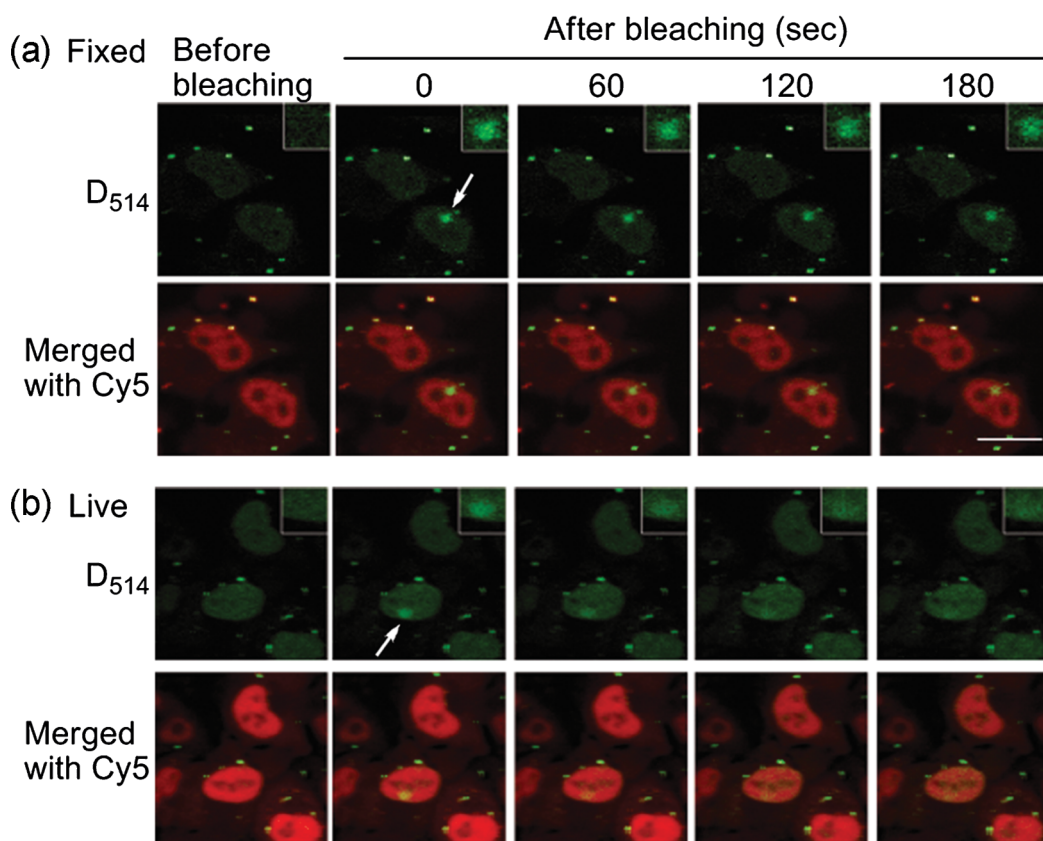


Fig. 5 Dynamic behaviour of poly(A)⁺ RNA in nucleoplasm. (a) HeLa cells fixed using 4% paraformaldehyde after transducing Cy5-s-s-U₂D₅₁₄U₁₉ probes before and after bleaching of Cy5. White arrows point to the photobleaching sites. Bar, 20 µm. (Insets) Extended images of the photobleaching site. (b) Living HeLa cells after transducing Cy5-s-s-U₂D₅₁₄U₁₉ probes before and after bleaching of Cy5.

fluorescence through a 625–722 nm filter when excited with a 488 nm Ar laser (red in Fig. 4b); the fluorescence was distributed in the nuclei, except in the nucleoli. This red fluorescence indicated the distribution of the probe after its injection into the cell. The fluorescence observed through a 505–550 nm filter (green) was weak, suggesting that the FRET process of Cy5-s-s-U₂D₅₁₄U₆ was active even in living cells. The nucleus of one of the probe-injected cells was then scanned repeatedly with a 633 nm He–Ne laser. The fluorescence observed through a red filter was lost only in the irradiated cell nucleus, suggesting that the Cy5 on the probe was photobleached and was no longer able to work as a FRET acceptor (Fig. 4c). Upon photobleaching of Cy5, the strong fluorescence of D₅₁₄, the FRET donor, was recovered through a green filter, indicating the location of the probe hybridized with the mRNA poly(A) tail.⁹

The acceptor bleaching system using binary photoprocess probes makes it possible to monitor the dynamic behavior of poly(A)⁺ RNAs in nucleoplasm. We focally bleached the Cy5 of Cy5-s-s-U₂D₅₁₄U₁₉ using repetitive illumination at a higher laser power (Fig. 5). A resultant increase in D₅₁₄ fluorescence was observed at the focal bleaching site (on average over 20 fold). Time-lapse images were taken in the next three minutes to follow the dynamic movement of focally labeled poly(A)⁺ RNA. In living HeLa cells, a rapid decrease of D₅₁₄ fluorescence at the focal site and a corresponding increase in entire nucleoplasm except for nucleoli, was observed (Fig. 5b). In control experiments, we fixed HeLa cells using 4% paraformaldehyde after transducing

Cy5-s-s-U₂D₅₁₄U₁₉ probes and conducted focal photobleaching of Cy5, where the fluorescence of D₅₁₄ remained constant at the photobleaching site and no apparent fluorescence spread in nucleoplasm was observed (Fig. 5a). This result is consistent with previous reports that poly(A)⁺ RNA move in a diffused fashion throughout the cytoplasm except for nucleoli.¹⁰

Conclusions

In conclusion, the fluorescence from oligonucleotides labeled with both ECHO nucleotides and a conventional fluorescent dye was controlled well by two intramolecular energy transfer processes, excitonic interaction and FRET. The controlled emission provided valuable information on the hybridization of the probe to RNA both *in vitro* and in the cell. It will be interesting to apply this technology to investigate the dynamics of nuclear poly(A)⁺ RNA processing and export under both physiological and diseased conditions in the future in order to understand the cellular pathology of human diseases.

Experimental

General

DNA was synthesized on an Applied Biosystems 392 DNA/RNA synthesizer or an NTS H-6 DNA/RNA synthesizer. Reversed-phase HPLC was performed on CHEMCOBOND 5-ODS-H

columns (10 × 150 mm) with a Gilson Chromatograph, Model 305, using a UV detector, Model 118, at 260 nm. MALDI-TOF mass spectra were measured with a Bruker Daltonics Reflex. UV and fluorescence spectra were recorded on a Shimadzu UV-2550 spectrophotometer and RF-5300PC spectrofluorophotometer, respectively.

Probe synthesis

Oligonucleotides containing 2'-*O*-methyluridine, Cy5, hexaethylene glycol spacer, and diamino- or monoamino-modified nucleotide were prepared by a standard phosphoramidite method on a DNA synthesizer. Phosphoramidites of 2'-*O*-methyluridine, Cy5, and hexaethylene glycol spacer were purchased from Glen research. Diamino- and monoamino-modified nucleoside phosphoramidites were synthesized according to our previous report.^{4b} The synthesized DNA oligomer was cleaved from the CPG support with 28% aqueous ammonia and deprotected according to the instruction of Cy5 phosphoramidite. After removal of ammonia from the solution under reduced pressure, the DNA was purified by reversed-phase HPLC, elution with a solvent mixture of 0.1 M triethylammonium acetate (TEAA) (pH = 7.0), and linear gradient over 20 min from 5% to 30% acetonitrile at a flow rate of 3.0 mL min⁻¹. A solution of the succinimidyl ester of thiazole orange dyes^{4b} (50 equiv to an active amino group of DNA) in DMF was added to a solution of purified DNA in 100 mM sodium carbonate buffer (pH = 9.0), and incubated at 25 °C for 10 min. The reaction mixture was diluted with ethanol. After centrifuging at 4 °C for 20 min, the supernatant was removed. The residue was dissolved in a small amount of water and then the solution was passed through a 0.45 μm filter. The product was purified by reversed-phase HPLC on a 5-ODS-H column, elution with a solvent mixture of 0.1 M TEAA (pH = 7.0), and linear gradient over 28 min from 5% to 40% acetonitrile at a flow rate of 3.0 mL min⁻¹. MMTr groups for protection of Cy5 were then removed according to the instruction of Cy5 phosphoramidite. The fluorescent DNA was identified by MALDI-TOF mass spectrometry.

Absorption and fluorescence measurements

Absorption and fluorescence spectra of the fluorescent probes (0.4 μM) were measured in 50 mM sodium phosphate buffer (pH = 7.0) containing 100 mM sodium chloride using a cell with a 1 cm path length. The excitation wavelength was 488 nm. The excitation and emission bandwidths were 1.5 nm.

Melting temperature measurements

The T_m values of duplexes (1.0 μM) were measured in 50 mM sodium phosphate buffer (pH = 7.0) containing 100 mM sodium chloride. The absorbance of the samples was monitored at 260 nm from 10 °C to 90 °C with a heating rate of 0.5 °C min⁻¹. From these profiles, first derivatives were calculated to determine the value of T_m .

Calculation of FRET efficiency

The transfer efficiency E was given by

$$E = 1 - (I_{DA}/I_D) \quad (1)$$

where I_{DA} and I_D are the fluorescence intensity of donor in the presence and absence of acceptor, respectively. E can also be written in the following form:

$$E = 1 / \{1 + (r/R_0)^6\} \quad (2)$$

where r is the donor-acceptor distance and R_0 is the Förster critical radius. R_0 can be written as

$$R_0 = 9.78 \times 10^2 (\kappa^2 n^{-4} Q_D J)^{1/6} \quad (3)$$

where J is the integral overlap, n is the average refractive index of the medium in the wavelength range, and Q_D is the fluorescence quantum yield of the donor in the absence of transfer. κ^2 is the orientational factor, which is usually taken to be 2/3. J is defined as

$$J = \int_0^\infty I_D(\lambda) \varepsilon_A(\lambda) \lambda^4 \delta \lambda \quad (4)$$

where λ is the wavelength in nm, $I_D(\lambda)$ is the fluorescence spectrum of the donor, and $\varepsilon_A(\lambda)$ is the molar absorption coefficient of acceptor in dm³ mol⁻¹ cm⁻¹. The J values calculated were 2.56×10^{-13} and 2.04×10^{-13} M⁻¹ cm³ for D₅₁₄/Cy5 and M₅₁₄/Cy5 systems, respectively.

Cell culture

Dulbecco's modified Eagle's medium (DMEM) and fetal bovine serum (FBS) were purchased from GIBCO. Reagents for culturing were from Sigma. HeLa cells were cultured at 37 °C in DMEM containing 10% heat-inactivated FBS, 25 U mL⁻¹ penicillin and 25 mg mL⁻¹ streptomycin, under a humidified atmosphere with 5% CO₂. For experimental use, cells (passage number 5–9) were cultured in glass-base dishes (Matsunami). Before microscope observation, the culture medium was washed and exchanged to phenol red-free DMEM. Cells were maintained in a culturing condition by an incubation system (INU; Tokai Hit) during observation.

Microinjection and acceptor bleaching

A probe Cy5-s-s-U₂D₅₁₄U₆ dissolved in water was microinjected using a pneumatic injector (FemtoJet express; Eppendorf) with glass needles (FemtoTip; Eppendorf) and 3-D manipulators (Narishige). Injection was performed at 130 hPa for 0.5 s in the cell (*ca.* 100–500 fL of 30 μM). Images were acquired with a motorized inverted microscope (Axio Observer Z1; Zeiss) equipped with an objective (PlanApochromat 63× oil immersion NA 1.4). Acquired images were analyzed and processed with Zeiss software (ZEN 2008, Zeiss). The probe was excited with 488 nm irradiation and detected through a filter of 505–550 nm for green and a filter of 625–722 nm for red. Subsequently, Cy5 of the probe was specifically bleached by the 633 nm HeNe laser line, set to 100% energy level using 200 bleaching cycles.

Transfection and acceptor bleaching

HeLa was transfected with Cy5-s-s-U₂D₅₁₄U₁₉ (25 μM) using Lipofectamine 2000 (Invitrogen). After incubation for 1 h in a probe/lipofectamine solution, the cells were rinsed twice with PBS and observed in phenol red-free DMEM. During observation and imaging, cells were maintained under culturing conditions

using a live-cell observation chamber system. Fixed cells were prepared using 4% paraformaldehyde in PBS at the end of the probe/lipofectamine incubation. Images were acquired on Axio Observer Z1 (Zeiss) with a PlanApochromat 63 \times oil immersion NA 1.4 objective. Fluorescence of D₅₁₄ was recorded using 514 nm excitation and 520–555 nm detection; FRET signal of Cy5 was recorded with 514 nm excitation and 660–730 nm detection. Focal acceptor bleaching was performed using a 633 nm HeNe laser (5 mW, 163.83 ms dwell time/pixel). Acquired images were processed and analyzed with ZEN 2008 (Zeiss).

Acknowledgements

We thank Dr Takehiro Suzuki (RIKEN) for the mass spectrometry.

Notes and references

- 1 B. Valeur, *Molecular Fluorescence: Principles and Applications*, Wiley-VCH, Weinheim, Germany, 2002.
- 2 B. W. van der Meer, G. Coker III and S.-Y. S. Chen, *Resonance Energy Transfer: Theory and Data*, VCH, New York, 1994.
- 3 (a) M. Kasha, *Radiat. Res.*, 1963, **20**, 55; (b) M. Kasha, H. R. Rawls and M. A. El-Bayoumi, *Pure Appl. Chem.*, 1965, **11**, 371; (c) G. L. Levinson, W. T. Simpson and W. Curtis, *J. Am. Chem. Soc.*, 1957, **79**, 4314; (d) E. G. McRae and M. Kasha, *J. Chem. Phys.*, 1958, **28**, 721.
- 4 (a) A. Okamoto, *Chem. Rec.*, 2010, **10**, 188; (b) S. Ikeda and A. Okamoto, *Chem.–Asian J.*, 2008, **3**, 958; (c) T. Kubota, S. Ikeda and A. Okamoto, *Bull. Chem. Soc. Jpn.*, 2009, **82**, 110; (d) S. Ikeda, M. Yuki, H. Yanagisawa and A. Okamoto, *Tetrahedron Lett.*, 2009, **50**, 7191.
- 5 T. Kubota, S. Ikeda, H. Yanagisawa, M. Yuki and A. Okamoto, *Bioconjugate Chem.*, 2009, **20**, 1256.
- 6 (a) R. F. Khairutdinov and N. Serpone, *J. Phys. Chem. B*, 1997, **101**, 2602; (b) L. D. Simon, K. H. Abramo, J. K. Sell and L. B. McGown, *Biospectroscopy*, 1998, **4**, 17; (c) G. Cosa, K.-S. Focsaneanu, J. R. N. McLean, J. P. McNamee and J. C. Scaiano, *Photochem. Photobiol.*, 2001, **73**, 585; (d) T. Sagawa, H. Tobata and H. Ihara, *Chem. Commun.*, 2004, 2090.
- 7 (a) S. Ikeda, T. Kubota, M. Yuki and A. Okamoto, *Angew. Chem., Int. Ed.*, 2009, **48**, 6480; (b) S. Ikeda, T. Kubota, K. Kino and A. Okamoto, *Bioconjugate Chem.*, 2008, **19**, 1719; (c) S. Ikeda, T. Kubota, M. Yuki, H. Yanagisawa, S. Tsuruma and A. Okamoto, *Org. Biomol. Chem.*, 2010, **8**, 546.
- 8 The M₅₁₄ in Cy5-s-s-U₁₅M₅₁₄U₆ also showed a hybridization-dependent fluorescence switching at 544 nm. It is not due to the control of interdyer excitonic interaction but just the control of the rotation around the methine bridge at the excited state.
- 9 T. Kubota, S. Ikeda, H. Yanagisawa, M. Yuki and A. Okamoto, *PLoS One*, 2010, **5**, e13003.
- 10 C. Molenaar, A. Abdulle, A. Gena, H. J. Tanke and R. W. Dirks, *J. Cell Biol.*, 2004, **165**, 191.